Stability of Fe/ZSM-5 de-NOx catalyst: effects of iron loading and remaining Brønsted acid sites

Ho-Taek Lee and Hyun-Ku Rhee *

School of Chemical Engineering and Institute of Chemical Processes, Seoul National University, Kwanak-ku, Seoul 151-742, Korea
E-mail: hkrhee@snu.ac.kr

Received 26 March 1999; accepted 26 May 1999

The stability of Fe/ZSM-5 de-NOx catalyst has been investigated. The samples are prepared by sublimation of iron chloride. Substantial amount of protons are found to remain in the fresh catalyst after washing and calcination. After 10 h exposure to wet exhaust gas at 600 °C, the catalyst is severely deactivated. The presence of steam induces dealumination of the ZSM-5 matrix, because the protons provide the point of attack by water. In addition, highly reactive distorted tetrahedral iron species and tetrahedral species change to less reactive octahedral iron ions or iron agglomerates upon aging treatment. With the second sublimation of iron chloride, the iron loading is increased and thus the concentration of remaining protons is reduced. Also, the catalyst turns out to preserve more reactive iron ions after aging treatment. In conclusion, the second sublimation is believed to bring about a remarkable improvement in the stability of the Fe/ZSM-5 catalyst although its de-NOx activity is slightly decreased.

Keywords: Fe/ZSM-5, steam treatment, deactivation, hydrothermal stability, SCR, de-NOx

1. Introduction

Metal-ion-exchanged ZSM-5 catalysts have been extensively studied for the selective catalytic reduction (SCR) of NOx under net oxidizing conditions by hydrocarbons. Nevertheless, application of these materials to the practical exhaust treatment appears to be a difficult task. One of the most important needs for the practical application of the SCR process is the durability of the catalyst.

In general, it has been found that the metal–zeolite catalysts deactivate irreversibly when exposed to a wet exhaust stream under high-temperature conditions. Many researchers have examined the stability of Cu/ZSM-5 to gain an insight into the effects of copper exchange level, additive addition, and the remaining protons [1–4]. The proton exchange site plays a crucial role in the Cu/ZSM-5 catalyst deactivation. It has been understood that wet condition induces dealumination of the zeolite matrix under high-temperature conditions and the copper states are irreversibly changed due to the interaction of copper with alumina formed during the dealumination process [1]. Tanabe et al. [2] claimed that the deactivation of Cu/ZSM-5 occurs through the migration of copper ions to the sites which reactant molecules cannot reach and that this migration is caused by the dealumination. A number of research works have been directed to the effect of additives on the stability of metal-loaded ZSM-5 [3,8]. However, it has not been successful in enhancing the stability to a satisfactory level.

Recently, a highly durable SCR catalyst, Fe/ZSM-5, has been reported by Feng and Hall [5]. The "over-exchanged" Fe/ZSM-5 catalysts were prepared by exchanging $[FeOH]^+$ ions into Na/ZSM-5 using a typical aqueous ion exchange method designed by these authors. They claimed that the catalyst showed high activity and selectivity in the SCR reaction and was not deactivated by wet exhaust gas stream under high-temperature excursion up to 800 °C. However, it was mentioned by the authors themselves that the results could not be reproduced [6].

Chen and Sachtler [7,8] proposed an easy-to-prepare Fe/ZSM-5, synthesized by subliming iron chloride into the cavities of H/ZSM-5. Iron loading up to Fe/Al = 1 was obtained for these samples. These authors reported that the performance of the catalyst was not impaired when 10% H_2O was added in the temperature range of 250–500 °C. By the sublimation of iron chloride, they prepared $[FeCl_2]^+$-loaded ZSM-5, in which all the ion exchange sites were charge balanced by iron species and the Brønsted acid sites disappeared completely. After washing and calcination, however, it was observed that some irons migrate out of the ion exchange sites to form iron oxides, and this induces the formation of a considerable amount of aluminum sites charge balanced with protons [8]. According to their report, Fe/ZSM-5 had protons in an amount equivalent to 20% of those from parent H/ZSM-5.

In this study, hydrothermal stability of Fe/ZSM-5 prepared by the sublimation method has been examined. To prepare the sample of higher iron loading and less proton sites, the method of repetitive sublimation has been adopted. The effects of the iron loading and the remaining protons on the stability of the samples have been discussed.

* To whom correspondence should be addressed.

2. Experimental

2.1. Sample preparation

Fe/ZSM-5 catalysts were prepared by the sublimation method as described by Chen and Sachtler [7]. Na/ZSM-5 ($SiO_2 : Al_2O_3 = 23.3$), supplied by Tosoh Corp., was ion-exchanged to NH_4/ZSM-5 and then calcined in an oxygen stream at 500 °C to give H/ZSM-5. Iron(III) chloride was sublimed into the cavities of the H/ZSM-5, in which it reacted chemically with a proton at a Brønsted acid site. After sublimation the resulting sample, the $[FeCl_2]^+$-loaded ZSM-5, was washed with doubly deionized water three times and then calcined at 500 °C in an oxygen stream for 2 h to give the sample Fe/ZSM-5-A.

Another sample to be called Fe/ZSM-5-B was prepared by applying a second sublimation of iron chloride to the sample Fe/ZSM-5-A followed by washing and calcination.

2.2. Catalyst deactivation

Deactivation was carried out in a simulated wet exhaust stream of NO (500 ppm), isobutane (500 ppm), O_2 (5%), H_2O (10%), and balance He. The catalysts were exposed to the stream at 600 and 700 °C, respectively, for 10 h.

2.3. Reaction experiment

A typical inlet gas was composed of 500 ppm NO, 500 ppm isobutane, 5% O_2, and balance He. The total flow rate was 200 ml/min and the catalyst weight was 0.20 g, which gave a GHSV of 30,000 h^{-1} based on the bulk density of 0.5 g/ml for the catalyst. The products were monitored by on-line gas chromatography (TCD detector, Porapak Q and Molecular Sieve 5A columns in sequence reversal configuration) and a chemiluminescence type NOx analyzer (Rosemount model 951A). The production of N_2O was below detection limit for both Fe/ZSM-5 samples. CO_2 and CO were detected as carbon product.

For the activity data report, we used two quantities defined as follows:

$$\text{NO conversion (\%)} = \left[(NO_{in} - NOx_{out})/NO_{in}\right] \times 100\%,$$

$$\text{Competitiveness factor (\%)} = \left[(NO_{in} - NOx_{out})/(13 \times i\text{-}C_4H_{10,consumed})\right] \times 100\%.$$

The competitiveness factor represents the ratio of the rate of hydrocarbon consumed to reduce NO to the rate of total hydrocarbon consumption.

2.4. Characterization

Temperature-programmed reduction (TPR) was carried out using a 12% H_2/N_2 mixture and heating from 20 to 900 °C with a ramping rate of 20 °C/min and holding at 900 °C for 20 min.

Table 1
Bulk and surface Fe/Al ratios and iron loadings of Fe/ZSM-5 catalysts after different treatments.

		Fe/ZSM-5-A			Fe-ZSM-5-B
		After sublimation	After washing and calcination	Aged at 700 °C	
Fe/Al	Bulk[a]		0.9		1.2
	Surface[b]	0.97	0.60	0.38	
Iron loading (wt%)	Bulk		5.2		7.1

[a] Determined by ICP analysis.
[b] Determined by XPS.

Electron spin resonance (ESR) spectra were taken in the X-band ($\lambda = 3.16$ cm) of the microwave region at 20 and –156 °C on a Bruker EMX spectrometer, equipped with ST cavity. The spectra were recorded at microwave power 0.1 mW and modulation amplitude 10 G in the field range of 400–4400 G. The sample (40 mg) was dehydrated in an oxygen stream at 500 °C for 2 h and transferred to the ESR sample tube. The tube was then sealed with a gas torch under vacuum without exposure to air.

Magic angle spinning (MAS) ^{27}Al nuclear magnetic resonance (NMR) spectra were taken on a Bruker DSX400 NMR spectrometer at 104.3 MHz with rotor spinning rate of 14 kHz, spectral width of 800 kHz, acquisition time of 0.0026 s, delay time of 4.0 s, and pulse length of 0.6 μs. All of the spectra were obtained at the same receiver gain.

Chemical analysis of the catalysts was undertaken by inductive-coupled plasma atomic emission spectroscopy (ICP-AES). X-ray photoelectron spectroscopy (XPS) measurements were performed on the pressed wafer of catalysts using a Kratos model AXIS-HS spectrometer.

Table 1 shows the values for both bulk and surface concentration ratios of Fe/ZSM-5 after each treatment.

3. Results

The TPR profiles of the Fe/ZSM-5 samples are presented in figure 1. These profiles show three H_2-consumption peaks at around 450, 600, and >800 °C. The first peak is assigned as the reduction of Fe^{3+} ions in the ion exchange sites of ZSM-5 to Fe^{2+} [7] as well as the reduction of Fe_2O_3 oxide to Fe_3O_4 [9]. The second peak corresponds to the reduction of Fe_3O_4 to Fe^0. Some of Fe^{2+} ions are irreversibly reduced to Fe^0 to give the last reduction peak [9].

The TPR result of Fe/ZSM-5-A, profile (a) in figure 1, shows two major peaks: one at 450 °C and the other at >800 °C. These peaks are attributed to the iron species in the ion exchange sites of ZSM-5. The small peak detected at 580 °C corresponds to the reduction of iron oxide particles. The profile of Fe/ZSM-5-B shows that iron loading is increased for both ionic species in the ion exchange sites and iron oxide particles. The first reduction peak of the sample is about 1.3 times larger than that of the

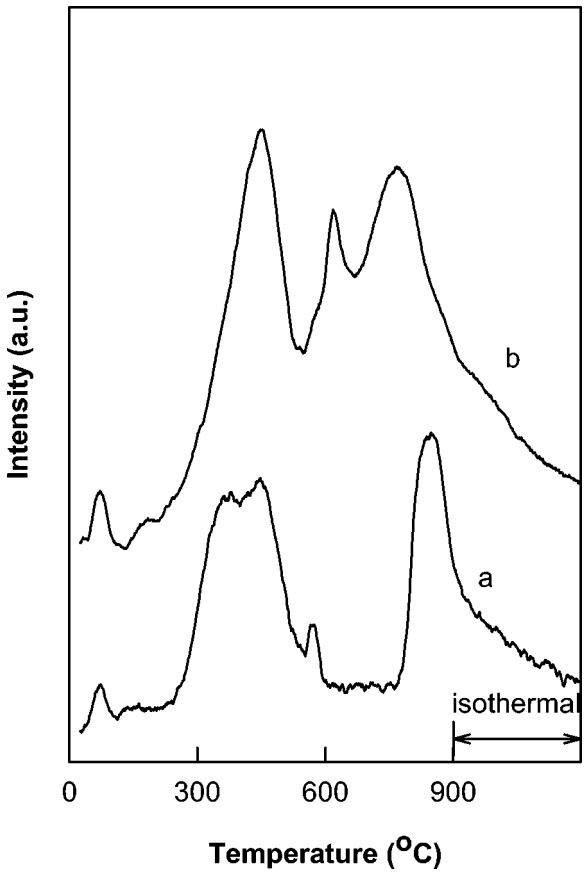

Figure 1. TPR profiles of Fe/ZSM-5 samples (a) prepared by the sublimation method (Fe/ZSM-5-A) and (b) modified by the second sublimation of iron chloride (Fe/ZSM-5-B).

Fe/ZSM-5-A sample, which is indicative of the increased amount of iron ions.

Figure 2 shows the infrared spectra in the hydroxyl stretching region of zeolite. Spectrum (a) shows two major hydroxyl peaks of the parent H/ZSM-5 at 3740 and 3610 cm^{-1}, which are assigned to the terminal silanol group and the Brønsted acidic hydroxyl group, respectively. Although it is not shown here, the spectrum taken right after the sublimation of iron chloride shows no peak in this region. Only after washing and calcination the peaks at 3740 and 3610 cm^{-1} appear again. As shown in spectrum (b) of figure 2 for the sample Fe/ZSM-5-A, the area of the Brønsted acidic hydroxyl peak at 3610 cm^{-1} decreases to about 30% of that obtained from the parent H/ZSM-5. In case of the sample Fe/ZSM-5-B, the peak is further reduced but a small amount of Brønsted acidic hydroxyl group still remained as observed in spectrum (c) of figure 2.

The ESR spectra of fresh Fe/ZSM-5 samples show four different lines, as depicted in figure 3, which are similar to those reported by Kucherov et al. [10,11]. They assigned these lines as follows: a weak line at $g = 2.0$ originating from octahedral Fe^{3+} ions and intense narrow lines in the low-field region from Fe^{3+} ions in tetrahedral ($g = 4.3$) and distorted tetrahedral ($g = 5.7$ and 6.5) coordinations. Characteristics of the iron oxide phase are represented by a very broad ESR line with $g = 2.2$, which is commonly formed in samples prepared by an aqueous ion exchange method.

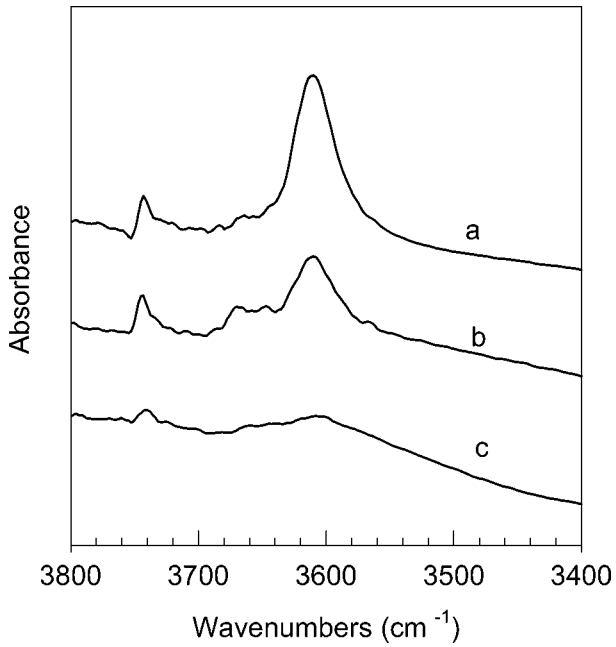

Figure 2. FTIR spectra in the –OH stretching region of (a) parent H/ZSM-5, (b) Fe/ZSM-5-A, and (c) Fe/ZSM-5-B.

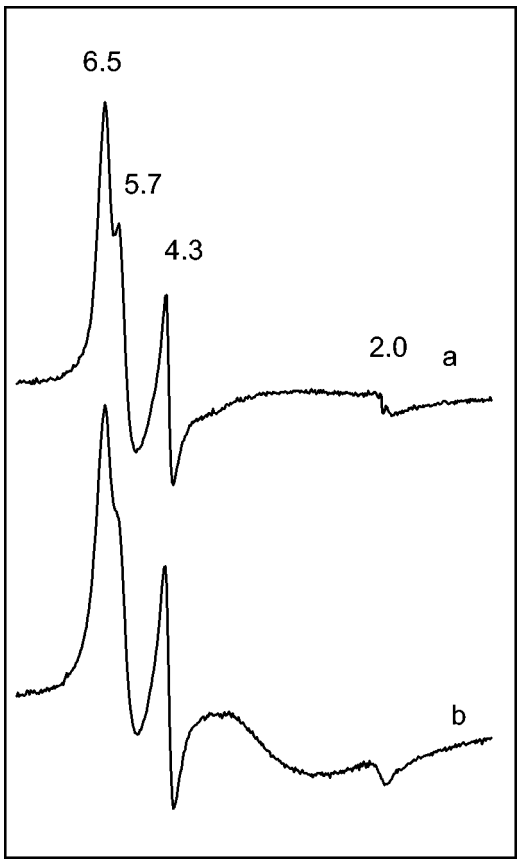

Figure 3. ESR signals, taken at $-156\,^{\circ}C$, of (a) fresh Fe/ZSM-5-A and (b) fresh Fe/ZSM-5-B.

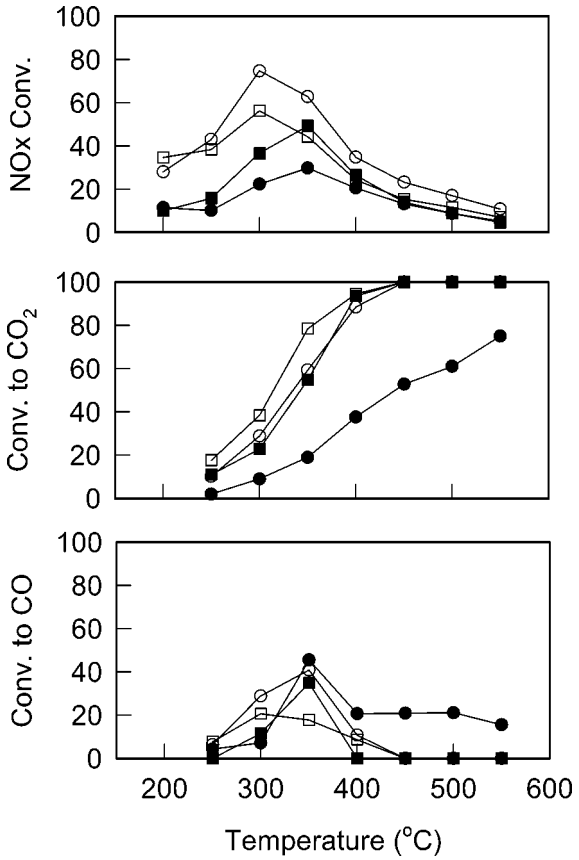

Figure 4. The effects of temperature on the SCR reaction over various Fe/ZSM-5 catalysts: (○) fresh Fe/ZSM-5-A, (●) Fe/ZSM-5-A aged at 600 °C, (□) fresh Fe/ZSM-5-B, and (■) Fe/ZSM-5-B aged at 600 °C.

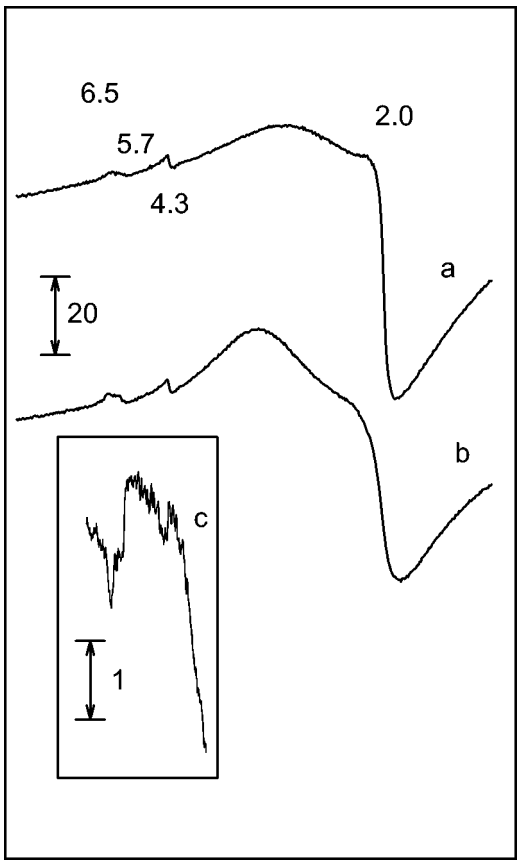

Figure 5. ESR spectra, taken at 20 °C, of two Fe/ZSM-5 samples after hydrothermal aging at 600 °C for 10 h: (a) Fe/ZSM-5-A, (b) Fe/ZSM-5-B, and (c) subtraction of spectrum (b) from spectrum (a).

Spectrum (a) of figure 3 indicates that most of the iron atoms in the fresh Fe/ZSM-5-A sample are present as tetrahedral or distorted tetrahedral ion species in the cationic positions of ZSM-5. This spectrum also shows that it contains very little iron oxide phase. It is well known that the low-field signal at $g = 5.7$ and 6.5 is associated with very reactive isolated Fe^{3+} cations in distorted tetrahedral coordination [10–12]. Thus, the concentration of this type of cations may be correlated with the reactivity of the catalyst. As indicated by the result of TPR analysis, ESR signals of Fe-ZSM-5-B (spectrum (b)) also show increased amounts of tetrahedral and distorted tetrahedral ion species in the cationic positions of ZSM-5. This is in good agreement with the IR results. The broad line of ferromagnetic resonance appearing in the spectrum represents the formation of iron oxide phase.

Figure 4 presents the results of the selective catalytic reduction of NOx over Fe/ZSM-5-A and Fe/ZSM-5-B. The results were taken over both fresh samples and those hydrothermally aged at 600 °C. With respect to the fresh samples, the de-NOx activity of Fe/ZSM-5-B is lower than that of Fe/ZSM-5-A, while the oxidation activity of the former is higher than that of the latter. Over the fresh Fe/ZSM-5-B, the yield of CO_2 is increased while that of CO is reduced.

However, Fe/ZSM-5-B is less sensitive to the hydrothermal deactivation. After aging at 600 °C for 10 h, Fe/ZSM-5-B maintained about 90% of its activity, though the maximum conversion temperature is shifted about 50 °C upward. In contrast, Fe/ZSM-5-A is severely deactivated after aging to give only less than 40% of its original activity.

Presented in figure 5 are the ESR spectra taken after hydrothermal aging at 600 °C. A strong broad line of ferromagnetic resonance and an overwhelmingly intense line at $g = 2.0$ appear, and the low-field ESR signal associated with the isolated iron ions weakens after the aging treatment. This implies that the reactive isolated ferric ions are changed to octahedral ferric ions or iron agglomerates. Comparing the low-field signals between the two Fe/ZSM-5 samples, we notice that the concentration of reactive distorted tetrahedral iron species is higher in Fe/ZSM-5-B than in Fe/ZSM-5-A.

The ^{27}Al MAS NMR spectra of the aged samples are presented in figure 6. Two signals at about 50 and 10 ppm have been assigned to framework and non-framework aluminum, respectively. Spectrum (a) clearly shows severe dealumination of Fe/ZSM-5-A. In the spectrum, the signal from the non-framework aluminum is more intense than that from the framework one. Spectrum (b) indicates that the aged Fe/ZSM-5-B preserves more framework aluminum. Though it also has some amount of non-framework species, the dealumination of the zeolite lattice occurs to a much lesser extent in Fe/ZSM-5-B.

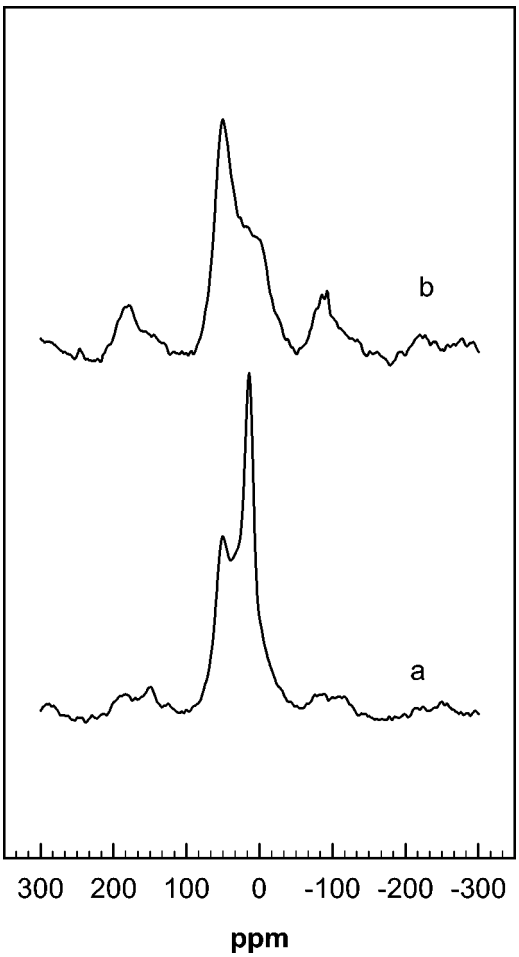

Figure 6. ^{27}Al MAS NMR spectra of (a) Fe/ZSM-5-A and (b) Fe/ZSM-5-B after hydrothermal aging at 600 °C for 10 h.

4. Discussion

4.1. Deactivation of Fe/ZSM-5

By adopting the sublimation method, we could prepare a Fe/ZSM-5 catalyst of high iron loading. After sublimation, Fe/Al = 1 is attained when the ion exchange rate was estimated by titration of the evolving HCl during the sublimation. In the resulting $[FeCl_2]^+$-loaded sample, no Brønsted acid site is detected by IR analysis of the hydroxyl stretching region, as all the ion exchange sites are occupied by the same number of iron ions.

After washing and calcination, however, a small amount of new protons was observed. This is the result of the hydrolysis of iron ions to neutral iron oxide particles and protons. The relative surface concentration of Fe/Al presented in table 1 indicates that iron oxide particles are formed after washing and calcination. Indeed, the bright yellow color of these $[FeCl_2]^+$-loaded catalysts changes to pale yellow after washing and to yellow with orange after calcination, which is also indicative of the formation of iron oxide particles. The resulting protons provide the point of attack by water molecules in the process of steam-induced dealumination and the dealumination of the zeolite matrix brings about the deactivation of Fe/ZSM-5. Therefore, it is evident that the concentration of remaining protons has a significant influence on the hydrothermal stability of the zeolite itself.

On the other hand, the aging treatment causes a significant change in the reactive iron species. The result of ESR analysis indicates that the reactive iron species change to less reactive octahedral ferric ions or to ferromagnetic iron agglomerates upon aging treatment. This is also confirmed by the XPS data presented in table 1. Though it is for the sample aged at 700 °C, the surface Fe/Al ratio is reduced from 0.6 to 0.38 after aging treatment while the change in the surface Si/Al ratio is negligible. This reduction is attributed to the formation of iron agglomerates. The formation of iron agglomerates has been also confirmed by Hall et al. [6], who conducted a Mössbauer spectroscopy study to observe the sextet splitting signal from a sample of "poor" Fe/ZSM-5. On the other hand, Kucherov et al. [11] reported that a mild reduction treatment also forms the ferromagnetic iron agglomerates.

4.2. Effects of second sublimation

The de-NOx activity of fresh Fe/ZSM-5-B was found lower than that of fresh Fe/ZSM-5-A, while the oxidation activity of the former is superior to that of Fe/ZSM-5-A. Though the former has more iron ions, it also has a considerable amount of iron oxide particles, as observed from the results of TPR and ESR analyses. Iron oxides are well known to catalyze the oxidation of hydrocarbons [13,14]. Direct combustion of hydrocarbon over these oxide particles reduces the selectivity for the selective reduction of NOx. Actually, the competitiveness factors at 300 °C are 10.0 for the fresh Fe/ZSM-5-A and 7.3 for the fresh Fe/ZSM-5-B, respectively. This indicates that the second sublimation of iron chloride reduces the usability of hydrocarbon as the NOx reducing agent.

Fe/ZSM-5-B turned out to be relatively stable under wet condition at high temperature. The major factor for the stability enhancement of Fe/ZSM-5-B is obviously the decrease in the concentration of remaining protons. As described in section 3, the amount of remaining proton sites is significantly reduced after the second sublimation, so the dealumination of zeolite lattice occurs to a much lesser extent in Fe/ZSM-5-B. According to the result of ESR analysis, it also preserves a larger amount of reactive distorted isolated iron than Fe/ZSM-5-A. When the concentration of remaining distorted tetrahedral species is estimated from the double integration of ESR spectra, the value for Fe/ZSM-5-B is 1.7 times larger than that of Fe/ZSM-5-A.

5. Conclusions

For Fe/ZSM-5 prepared by sublimation of iron chloride, steam-induced dealumination is one of the major causes of deactivation when exposed to a wet exhaust stream un-

der high-temperature conditions. In addition, highly reactive distorted tetrahedral iron species and tetrahedral species change to less reactive octahedral ferric ions or to iron agglomerates upon aging treatment. The second sublimation of iron chloride increases the iron loading and decreases the concentration of remaining protons, which provide the point of attack by water in the dealumination process. It is also found that the second sublimation of iron chloride makes the catalyst preserve more reactive distorted isolated iron after aging treatment. Consequently, the stability of the catalyst is remarkably improved although the de-NOx activity of this catalyst is slightly lower than that of the unmodified Fe/ZSM-5.

Acknowledgement

The authors gratefully acknowledge the financial support of the SK Corporation. The authors are also indebted to Professor Sa-Ouk Kang of the Research Center for Molecular Microbiology, Seoul National University, for ESR measurements.

References

[1] J.Y. Yan, G.D. Lei, W.M.H. Sachtler and H.H. Kung, J. Catal. 158 (1996) 327.
[2] T. Tanabe, T. Iijima, A. Koiwai, J. Mizuno, K. Yokota and A. Isogai, Appl. Catal. B 6 (1995) 145.
[3] P. Budi, E. Curry-Hyde and R.F. Howe, Catal. Lett. 41 (1996) 47.
[4] C. Torre-Abreu, M.F. Ribeiro, C. Henriques, F.R. Ribeiro and G. Delahay, Catal. Lett. 43 (1997) 31.
[5] X. Feng and W.K. Hall, J. Catal. 166 (1997) 368.
[6] W.K. Hall, X. Feng, J. Dumesic and R. Watwe, Catal. Lett. 52 (1998) 13.
[7] H.Y. Chen and W.M.H. Sachtler, Catal. Today 42 (1998) 73.
[8] H.Y. Chen and W.M.H. Sachtler, Catal. Lett. 50 (1998) 125.
[9] Y. Okamoto, H. Kikuchi, Y. Ohto, S. Nasu and O. Terasaki, Stud. Surf. Sci. Catal. 105 (1997) 2051.
[10] A.V. Kucherov and A.A. Slinkin, Zeolites 8 (1988) 110.
[11] A.V. Kucherov, C.N. Montreuil, T.N. Kucherova and M. Shelef, Catal. Lett. 56 (1998) 173.
[12] J. Varga, J. Halasz, D. Horvath, D. Mehn, J.B. Nagy, G. Schobel and I. Kiricsi, Stud. Surf. Sci. Catal. 116 (1998) 367.
[13] M. Baldi, V.S. Escribano, J.M.G. Amores, F. Milella and G. Busca, Appl. Cat. B 17 (1998) L175.
[14] K. Masahito, Eur. Patent 0 600 442 A1 (1994), to Nippon Shokubai Co.